Published in final edited form as:

*FASEB J.* 2020 March ; 34(3): 4219–4233. doi:10.1096/fj.201901511R.

# Differential regulation of macrophage activation by the MIF cytokine superfamily members MIF and MIF-2 in adipose tissue during endotoxemia

**Bong-Sung Kim**[1,2,3,*,+], **Pathricia V. Tilstam**[1,*,+], **Kevin Arnke**[3], **Lin Leng**[1], **Tim Ruhl**[2], **Marta Piecychna**[1], **Wibke Schulte**[1,4,5,6], **Maor Sauler**[7], **Florian S. Frueh**[3], **Gabriele Storti**[8], **Nicole Lindenblatt**[3], **Pietro Giovanoli**[3], **Norbert Pallua**[2], **Jürgen Bernhagen**[9,10], **Richard Bucala**[1]

[1]Department of Internal Medicine, Yale University School of Medicine, New Haven, CT [2]Department of Plastic, Reconstructive and Hand Surgery, RWTH Aachen University, Aachen, Germany [3]Department of Plastic Surgery and Hand Surgery, University Hospital Zurich, Switzerland [4]Department of Surgery, Yale University School of Medicine, New Haven, CT [5]Department of Surgery, Campus Charité Mitte | Campus Virchow-Klinikum, Charité – Universitätsmedizin Berlin, Berlin, Germany [6]Berlin Institute of Health (BIH), Berlin, Germany [7]Department of Pulmonary, Critical Care, and Sleep Medicine, Yale University School of Medicine, New Haven, CT [8]Unit of Plastic and Reconstructive Surgery University of Rome- "Tor Vergata" [9]Department of Vascular Biology, Institute for Stroke and Dementia Research, Ludwig-Maximilians-University Munich, Munich, Germany [10]Munich Cluster for Systems Neurology, 81377 Munich, Germany

## Abstract

Sepsis is a leading cause of death worldwide and recent studies have shown white adipose tissue (WAT) to be an important regulator in septic conditions. In the present study, the role of the inflammatory cytokine macrophage migration inhibitory factor (MIF) and its structural homolog *D*-dopachrome tautomerase (D-DT/MIF-2) were investigated in WAT in a murine endotoxemia model. Both MIF and MIF-2 levels were increased in the peritoneal fluid of LPS-challenged wildtype mice, yet in visceral WAT, the proteins were differentially regulated, with elevated MIF but down-regulated MIF-2 expression in adipocytes. *Mif* gene deletion polarized adipose tissue macrophages (ATM) towards an anti-inflammatory phenotype while *Mif-2* gene knockout drove ATMs towards a pro-inflammatory phenotype and *Mif*-deficiency was found to increase fibroblast

[+]Co-corresponding Authors: Bong-Sung Kim, MD, Universitätsspital Zürich, Klinik für Plastische Chirurgie und Handchirurgie, Rämistrasse 100, 8091 Zürich, Tel.: +41 44 255 27 38, bong-sung.kim@usz.ch, bong.kim@rwth-aachen.de, Pathricia V. Tilstam, PhD, Yale University School of Medicine, Internal Medicine/ Rheumatology Department, PO Box 208031, 300 Cedar Street, New Haven, CT 06520-8031, Tel.: +1- 203.737.5103, pathricia.tilstam@yale.edu.

[*]equal contribution

Author contributions

Study conception and design: B.S. Kim, J. Bernhagen, R. Bucala, P.V. Tilstam

Acquisition of data: B.S. Kim, P.V. Tilstam, M. Piecychna, W. Schulte, L. Leng, T. Ruhl, G. Storti

Analysis and interpretation of data: B.S. Kim, P.V. Tilstam, K. Arnke, M. Sauler, F. S. Frueh, N. Lindenblatt, P. Giovanoli, N. Pallua, J. Bernhagen, R. Bucala

Drafting of manuscript: B.S. Kim, P.V. Tilstam, K. Arnke, F. S. Frueh, G. Storti

Critical revision: L. Leng, T. Ruhl, W. Schulte, M. Sauler, N. Lindenblatt, O. El Bounkari, P. Giovanoli, N. Pallua, J. Bernhagen, R. Bucala

Final approval of the submitted manuscript: all authors.

viability. Additionally, we observed the same differential regulation of these two MIF family proteins in human adipose tissue in septic *vs* healthy patients. Taken together, these data suggest an inverse relationship between adipocyte MIF and MIF-2 expression during systemic inflammation, with the downregulation of MIF-2 in fat tissue potentially increasing pro-inflammatory macrophage polarization to further drive adipose inflammation.

**Keywords**

MIF; MIF-2; D-DT; adipose tissue; inflammation; macrophage; sepsis; wound healing; macrophage polarization

## Introduction

Sepsis is a fatal disease that, despite significant research attention, continues to affect hospitalized patients irrespective of age, ethnicity, or medical pre-condition (1, 2). In 1992 the American College of Chest Physicians (ACCP) and the Society of Critical Care Medicine (SCCM) released a consensus attempting to define and categorize sepsis, which was revised in 2014/2015 and published as the Third International Consensus Definitions for Sepsis and Septic Shock (3, 4). Despite the consensus and substantial improvements in supportive care, sepsis remains a major challenge to modern surgical research and is a public health concern; even those fortunate to survive, develop significant medical problems, as well as social and financial burden on health care systems (5, 6). While the detrimental effect of sepsis on organs such as heart, kidney, lungs, and their respective responses have been investigated in detail over the years, attention has been more recently directed on the role of white adipose tissue (WAT). An increasing body of literature underscores special functions of adipose tissue in inflammation and sepsis. In septic patients, adipose tissue alters cytokine expression to promote the inflammatory response and influences the macrophage phenotype towards a pro-inflammatory polarization (7, 8). On the other hand, recent meta-analyses by Pepper *et al.* and Wang *et al.* indicate a potential protective role of adipose tissue in critical illness, as overweight/obese patients show better outcome when compared to lean patients under septic conditions (9, 10). However, the molecular reasons for this “obesity paradox” remain unknown (11). On the cellular level, adipose tissue macrophages (ATMs) may be an important immunological cell type in septic conditions as they are the predominant leukocyte population in adipose tissue (12). ATMs are believed to initiate and regulate inflammation in adipose tissue by secreting diverse soluble factors.

The macrophage migration inhibitory factor (MIF) protein superfamily consists of the cytokine MIF (more recently also termed MIF-1) and its homolog D-dopachrome tautomerase (D-DT, also called MIF-2). Both members are abundantly expressed in adipose tissue (13, 14). MIF and MIF-2 are involved in the pathogenesis of sepsis as evidenced by the fact that both proteins are highly expressed in systemic inflammation and by the observation that anti-MIF or anti-MIF-2 protect mice from lethal endotoxemia (15–17). However, there is evidence to suggest an inverse relationship in the expression and action of MIF and MIF-2 in obesity and chronic adipose tissue inflammation (18). In contrast to MIF, MIF-2 shows a negative correlation with obesity and may ameliorate insulin resistance (19).

We have shown recently that MIF and MIF-2 are differentially expressed in subcutaneous adipose tissue from patients with inflamed chronic wounds and exert inverse action in wound repair *in vitro* (20, 21). In LPS-injected adipose tissue, MIF induced macrophage migration whereas MIF-2 had no such effect (20).

In the present study, we investigated the expression of MIF and MIF-2 in visceral WAT (vWAT) during LPS-induced endotoxemia in lean mice and examined the impact of *Mif* and *Mif-2* gene knockout on adipose tissue macrophage (ATM) polarization. We further performed assays on MIF/MIF-2-dependent fibroblast viability *in vitro* to shed light on the functional role of adipose MIF and MIF-2. Based on our prior studies with human adipose tissue samples in the context of adipose tissue inflammation during wound healing, we hypothesized that we would observe a similar inverse expression of MIF and MIF-2 in adipose tissue during LPS-induced endotoxemia with differential action on macrophage phenotypes.

## Methods

### Experimental animals

Eight to 12-week-old male C57BL/6 wildtype (WT), male *Mif*$^{-/-}$, and male *Mif-2*$^{-/-}$ mice were used in this study. WT mice were purchased from Charles River Laboratory (Wilmington, United States). *Mif*$^{-/-}$ mice were maintained in the pure C57BL/6J background as described previously (22). Constitutive *Mif-2*$^{-/-}$ mice lacking the entire *Mif-2* gene (promoter and 3 exons) were generated by Cre-mediated genomic deletion of a previously described Mif-2-flox mouse (23). Briefly, genomic DNA containing *Mif-2* was isolated from a C57BL/6J RPCIB-731 BAC library and a *Mif-2* targeting vector was designed to replace the *Mif-2* exons 1 and 2 with flanking *loxP* sequences for Cre recombination. The final targeting vector was additionally flanked with 5′ and 3′ arms containing genes for puromycin resistance and tyrosine kinase and transfected into the C57BL/6N Tac embryonic stem cell line. A combined positive and negative selection strategy (puromycin, ganciclovir) eliminated the untargeted and non-homologous recombinant ES cells. Homologous recombinants were selected by Southern blot analysis and the targeted ES clones verified by sequencing prior to microinjection into blastocysts. Chimeric mice with germline transmission were identified and offspring bred to homozygosity in the pure C57BL/6 mice in the Yale School of Medicine animal facility. Animals were housed in plastic cages and access to food and water *ad libitum*. Yale University's Institutional Animal Care and Use Committee approved all animal experiments (2015–10756/ 2017–10992).

### Statistical significance

GraphPad Prism software (San Diego, CA) was used for statistical analysis. Unless indicated otherwise, results are expressed as mean values ± SEM. Normal distribution was tested by the Kolmogorov-Smirnov test. For normally distributed data, statistical significance was determined by unpaired two-tailed Student's *t*-test or by one-way ANOVA followed by Bonferroni's multiple comparison test. For datasets with no normal distribution, statistical

significance was calculated by the Mann-Whitney test or Kruskal-Wallis test with Dunn's multiple comparison test. * $p < 0.05$, ** $p < 0.01$, *** $p < 0.001$, **** $p < 0.0001$.

### Induction of endotoxemia

10 mg/kg of LPS from *Escherichia coli* (*E. coli* O111:B4) (Sigma Aldrich, St. Louis, United States) was injected into the peritoneum of WT, *Mif*$^{-/-}$, and *Mif-2*$^{-/-}$ mice. Control mice were treated with the same volume of sterile phosphate buffered saline (1x PBS, Gibco, Thermo Fisher Scientific). Mice were sacrificed after 6, 12, 18, 24, 48, and 72 hours, and peritoneal lavage as well as adipose tissue were harvested for further analysis.

### Isolation of peritoneal macrophages and peritoneal lavage

Peritoneal macrophages (PMs) and intraperitoneal fluid were collected from euthanized mice by peritoneal lavage with 10 ml PBS and centrifuged at 300 g for 5 minutes. The supernatants were collected for protein measurement and stored at −20 °C. The remaining cell pellet containing the PMs was treated with ammonium-chloride-potassium (ACK) lysis buffer (Lonza, NJ, USA) for erythrocyte lysis. The cells then were washed, centrifuged, and counted in a Countess® II Automated Cell Counter (Thermo Fisher Scientific, MA, USA) with dead cells excluded by trypan blue, and then used for further experiments. PMs were characterized in two separate subsets by flow cytometric analysis. Briefly, cells were labeled at 4 °C for 30 min in FACS Buffer with the following fluorophore-conjugated antibodies: CD11b-AlexaFluor700 (eBioscience, CA, United States), F4/80-eFluor450 (eBioscience, CA, United States), CD45-APC-Cy7 (BD Pharmingen, CA, United States). Flow cytometry was performed on a LSR II cytometer (Becton Dickinson, Franklin, NJ) and analyzed with Flow Jo software (Tree Star, Ashland, OR). We characterized the different PM subsets as F4/80$^{high}$, CD11b$^{+}$ or F4/80$^{low}$, CD11b$^{+}$.

### Isolation of adipose tissue, stromal vascular fraction, and adipocytes

Depending on the experiment, either whole vWAT (before enzymatic digestion) or stromal vascular fraction (SVF) and adipocytes (after enzymatic digestion) were isolated as described previously (24). Briefly, after cardiac perfusion with 10 ml PBS, vWAT was excised with meticulous removal of lymph nodes and other non-adipose tissue. Explants were washed with PBS twice, minced with scissors, and digested with collagenase (Collagenase type II, Sigma-Aldrich, MO, USA) to separate adipocytes from SVF cells. Digested tissue was incubated with 2 mM ethylenediaminetetraacetic acid (EDTA, AmericanBio, Inc., MA, USA), filtered through a 100 μm mesh, and centrifuged at 500 g for 10 minutes. Floating adipocytes were transferred into separate tubes and either cultivated or immediately assayed. The SVF-containing cell pellet underwent erythrocyte lysis in ACK lysis buffer, was washed and pelleted by centrifugation, and finally either put into culture or used for further downstream application.

### LPS stimulation of cultured adipocytes and SVF cells *in vitro*

Isolated adipocytes and SVF cells were cultured in Dubeccos's modified Eagle's medium (DMEM, supplemented with 10% FCS, 25 mmol/l HEPES, 10 000 U penicillin/ml, 10 mg/ml streptomycin) in a humidified 37 °C, 5% $CO_2$ incubator. After one day of culture,

adipocytes were removed from the culture flask to separate adipocytes from adherent fibroblasts (25). Two days after adipocyte and SVF cell isolation, cells were stimulated with 0.01 – 100 μg/ml LPS for 48 hours. After stimulation, cells were lysed, and lysates were used for MIF and MIF-2 ELISA. Supernatants were collected after PBS and LPS stimulation to use for *in vitro* polarization of isolated murine WT and *Mif-2*$^{-/-}$ bone marrow-derived macrophages (BMDM). To minimize adipocyte contamination in the supernatants, adipocytes were stimulated in cell inserts with a pore-size of 0.4 μm (Merck Millipore, MA, USA).

### Harvest and *in vitro* polarization of bone marrow-derived macrophages

BMDMs from sacrificed WT and *Mif-2*$^{-/-}$ mice were harvested from femoral and tibial bone marrow by cutting the proximal and distal end of each bone and flushing with sterile PBS. Collected cells were centrifuged at 300 g for 5 minutes and cultured in growth medium (RPMI-1640, 15% L929-conditioned medium (CM), 10% FCS, 10,000 U penicillin/ml, 10 mg/ml streptomycin) for seven days. L929-CM was generated following a standardized protocol (26). After seven days, BMDMs were treated with supernatants from PBS and LPS-stimulated WT and *Mif-2*$^{-/-}$ adipocytes and SVF cells mixed with starvation medium (90% RPMI, 5% FBS, 5% L929-CM, 10 000 U penicillin/ml, 10 mg/ml streptomycin). After 48 hours, macrophage phenotype was assessed by flow cytometry.

### Macrophage phenotype analysis by flow cytometry

Adipose tissue macrophages (ATM) and their respective pro- or anti-inflammatory phenotype markers were characterized by flow cytometry as described earlier (24). SVF cells were stained with the following antibodies: CD11b-AlexaFluor700 (eBioscience, CA, United States), F4/80-eFluor450 (eBioscience, CA, United States), CD45-APC (Biolegend, CA, United States), CD11c-PE, CD301-AlexaFluor647 (AbD Serotec, NC, USA). All samples were measured on a LSR II cytometer (BD Bioscience, CA, USA) and the data was analyzed by FlowJo (OR, United States). After exclusion of singlets by forward and sideward scatter, macrophages were defined as CD45$^{+}$, CD11b$^{+}$, F4/80$^{+}$ cells. CD11c was used as a pro-inflammatory macrophage marker, while CD301 served as an anti-inflammatory marker. To characterize intracellular protein levels of pro-and anti-inflammatory markers, SVF fraction cells were surface-stained with CD11b-AlexaFluor700 (eBioscience, CA, United States), F4/80-eFluor450 (eBioscience, CA, United States), CD45-APC-Cy7 (BD Pharmingen, CA, United States) and then fixed and permeabilized with Fix/Perm Buffer (eBioscience FoxP3/Transcription Factor Buffer Set, Invitrogen/ Thermo Fisher Scientific, CA, United States) according to manufacturer's instructions. After fixation and permeabilization, the cells were stained intracellularly for MCP1-APC (R&D Systems, MN, United States), TNFα-PE (eBioscience, CA, United States), Arginase1-FITC (R&D Systems, MN, United States) and TGFβ-PerCP-Cy5.5 (Biolegend, CA, United States). All samples were measured on an LSR II cytometer (BD Bioscience, CA, USA) and the data was analyzed by FlowJo (OR, United States). Adipose tissue macrophages were defined as CD45$^{+}$, CD11b$^{+}$, F4/80$^{+}$ cells and then further analyzed for intracellular expression of the pro-inflammatory markers MCP1 and TNFα as well as the anti-inflammatory markers TGFβ and Arginase1.

### Protein measurement and MIF/ MIF-2 ELISA

Total protein content was measured by the Pierce™ BCA Protein Assay Kit (ThermoFisher, MA, USA) following to the manufacturer's instructions. Absorbance was detected at 560 nm using an iMark Microplate Absorbance Reader (Bio-Rad Laboratories, Inc., CA, USA). MIF and MIF-2 levels of whole adipose tissue samples were measured by ELISA and normalized to the total protein contents. Briefly, to analyze mouse MIF levels, plates were coated with a monoclonal anti-mouse capture antibody XIV.14.3 (purified anti-mouse MIF mono IgG1, 15 μg/mL) diluted in 1 x PBS and incubated overnight at 4°C and the following day after washing the plate, the plates were blocked using 1x ELISA diluent (eBioscience, CA, United States) overnight at 4 °C. On the following day, the excess blocking buffer was removed. The coated wells were loaded with samples and recombinant mouse MIF as standard (prepared in ELISA Diluent, range 0–100 ng/mL) and incubated overnight at 4 °C. Next day, wells were washed and treated with a polyclonal goat secondary antibody diluted in ELISA diluent (sc-16965, Santa Cruz, CA, USA) and incubated for 2 hours at room temperature. Afterwards the wells were washed and incubated with a polyclonal bovine anti-goat IgG-horse radish peroxidase (HRP) detection antibody (sc-2350, Santa Cruz, CA, USA) diluted in ELISA diluent for 1 hour at room temperature. After washing, the plates were developed with TMB Substrate Solution (Dako, CA, USA) in the dark and the reaction stopped by stop solution (0.5 M $H_2SO_4$ - 0.5 M HCl). Plates were read at 450/590 nm with an iMark Microplate Absorbance Reader. MIF-2 levels were measured by ELISA as reported previously (16). All ELISA measurements were run in duplicates.

### Quantitative real time-polymerase chain reaction (RT-PCR)

The mRNA for RT-PCR was prepared by the RNeasy Mini Kit (Qiagen, CA, USA) and cDNA synthesized with the Quantitect® Reverse Transcription Kit (Qiagen, CA, USA) following the manufacturer's instructions. Quantitative RT-PCR was performed with the iTaq™ Universal SYBR Green Supermix (Bio-Rad Laboratories, Inc., CA, USA) on a C1000™ Thermal Cycler (Bio-Rad Laboratories, Inc., CA, USA). Primers used are listed in Table 1. The housekeeping gene *β-actin* served as an internal control for normalizing murine gene expression. Data were analyzed with the comparative cycle time (CT) method by calculating the ΔCT as the difference in cycle times between the tested gene and housekeeping gene. Next, the ΔΔCT was obtained by determination of the difference between the control and experimental conditions. All RT-PCR measurements were done in triplicates.

### Co-culture with 3T3 fibroblasts and proliferation assay

First, 50,000 3T3 fibroblasts were seeded in 24 well plates overnight. The following day, fibroblasts were co-cultured with 0.3 g vWAT isolated from *Mif*$^{-/-}$, *Mif-2*$^{-/-}$ and WT mice after LPS injection. Adipose tissue and fibroblasts were separated by cell inserts with a pore-size of 0.4 μm (Merck Millipore, MA, USA). One ml growth medium containing 0.5% FCS was added. Medium with 0.5% FCS and 10% FCS and no additional adipose tissue served as negative and positive control. To assess fibroblast proliferation alamarBlue® assay (Thermo Fisher Scientific, Waltham, Massachusetts, USA) was performed before addition of vWAT as well as one day after addition of vWAT samples.

### MIF and MIF-2 ELISA from subcutaneous WAT samples of septic patients

Subcutaneous WAT (sWAT) was collected from ten patients with Gram-negative bacterial sepsis. The ethics committee of the RWTH Aachen University approved the study with human samples (EK 163/07), written consent was provided by each patient. Sepsis was defined according to the ACCP/SCCM consensus conference criteria (27). Ten matched healthy patients served as controls. Adipose tissue was homogenized, and human MIF-2 ELISA and human MIF ELISA were performed as described previously (16, 21).

## Results

### Peritoneal MIF and MIF-2 levels increase under endotoxemia

We used an established LPS shock model to induce endotoxemia for investigating the role of MIF and MIF-2 in septic conditions. After *i.p.* injection of 10 mg/kg LPS into WT mice, intraperitoneal fluid was collected after 6, 12, 18, 24, 48, and 72 hours (n=8 per time point). PBS injected WT mice served as controls (n=8). MIF levels were elevated after 6 hours and levels peaked additionally again after 24 (significant) and 48 hours when compared to the control group (Fig. 1A). MIF-2 levels also were significantly elevated after 24 hours (Fig. 1B). Notably, MIF-2 levels were significantly lower in both the control as well as the LPS-challenged group, when compared to the respective MIF levels (Fig. 1A, B). Additionally, we measured *Mif* and *Mif-2* mRNA expression levels in peritoneal macrophages (PMs). After *i.p.* injection of 10 mg/kg LPS into WT mice, PMs were collected after 6, 12, 24 and 48 hours (n=9 per time point) and PBS-injected WT mice served as controls (n=9). We observed *Mif* mRNA expression to be significantly elevated after 6 hours of *i.p.* LPS-treatment and then to decline after 12 hours of treatment, while *Mif-2* expression remained at similar levels to the PBS-treated control group at 6 hours of treatment but decreased after 12 hours post-LPS-injection (Supplementary Fig. S1). This data suggest that PMs may be a crucial source for peritoneal MIF especially at the early onset of the inflammation, while peritoneal MIF-2 may be secreted by a different cellular source.

### MIF and MIF-2 expressions are conversely regulated in vWAT

We measured MIF and MIF-2 protein levels and mRNA expression from homogenized vWAT following LPS injection after 6, 12, 18, 24, 48, and 72 hours (n=8) with PBS injected WT mice serving as controls. While MIF protein as well as mRNA levels increased after LPS challenge in vWAT (Fig. 1C, E), MIF-2 protein and mRNA expression were significantly reduced in vWAT after LPS challenge when compared to the control group (Fig. 1D, F).

### MIF-2 expression in adipocytes but not the stromal vascular fraction is decreased upon LPS challenge

Adipose tissue consists of various cell types including mature adipocytes and SVF cells which include adipogenic progenitor cells, ATMs, fibroblasts, pericytes, and many more. To identify the cellular source responsible for the differential MIF and MIF-2 expression in vWAT during endotoxemia, we isolated adipocytes as well as SVF from vWAT of LPS-challenged mice (n=8) and analyzed the MIF and MIF-2 levels. After LPS injection,

adipocytes showed no differential MIF levels in endotoxemia compared to the control group (Fig. 2A), the SVF cells exhibited increased MIF levels compared to PBS control group (Fig. 2B). However, during endotoxemia MIF-2 levels were significantly lower in adipocytes (Fig. 2C), but no changes in MIF-2 levels were observed in SVF cells compared to the control group (Fig. 2D).

We confirmed these findings by *in vitro* LPS-stimulation of vWAT-isolated adipocytes (n=6) and SVF cells (n=6) from untreated WT mice. In SVF cells, we observed MIF levels to rise with increasing LPS concentration (Fig. 3A), while cultured adipocytes stimulated with LPS did not show any altered MIF protein expression when compared to PBS-stimulated controls (Fig. 3B). Similar as the MIF expression, SVF cells showed a significant increase of MIF-2 levels at LPS concentrations of 10 μg/ml and 100 μg/ml (Fig. 3C). MIF-2 levels in adipocytes by contrast, diminished when cultured with 10 μg/ml and 100 μg/ml of LPS compared to PBS control (Fig. 3D).

## MIF induces a pro-inflammatory phenotype in ATMs while MIF-2 promotes an anti-inflammatory phenotype

We next sought to elucidate the role of adipose MIF and MIF-2 expression on the ATM phenotypes during endotoxemia. WT, *Mif*$^{-/-}$ and *Mif-2*$^{-/-}$ mice (n=10 each group) were challenged with LPS, vWAT harvested and ATM phenotype was characterized by flow cytometric analysis of the surface markers CD11c (pro-inflammatory) and CD301 (anti-inflammatory) as reported earlier (24). In the control group, mice were injected with PBS. The distribution of pro- and anti-inflammatory phenotypes in ATMs was expressed by an CD11c/CD301-ratio and we observed the CD11c/CD301-ratio of ATMs in LPS-treated *Mif*$^{-/-}$ mice to be significantly reduced when compared to WT mice (Fig. 4A, B) indicating a shift into a larger population of anti-inflammatory ATMs, while ATMs of LPS-treated *Mif-2*$^{-/-}$ mice exhibited elevated levels of a pro-inflammatory phenotype demonstrated by a significant increase of the CD11c/CD301-ratio compared to WT mice (Fig. 4C, D). Additionally, we analyzed the mRNA expression of both pro-and anti-inflammatory cytokines in vWAT after LPS injection in WT, *Mif*$^{-/-}$ and *Mif-2*$^{-/-}$ mice (n=8 each group). The expression levels of the pro-inflammatory cytokines *Tnfα* and *Mcp1* were decreased in *Mif*$^{-/-}$ mice (Fig. 4E, F), whereas the anti-inflammatory cytokine *Tgfβ* mRNA levels were upregulated in vWAT from *Mif*$^{-/-}$ mice when compared to WT mice (Fig. 4G, H). The expression of *Tnfα* and *Mcp1* in vWAT from LPS-injected *Mif-2*$^{-/-}$ mice on the other hand was up-regulated (Fig. 4I, J), whereas the mRNA expression of *Arg1*, a binuclear manganese metalloenzyme and marker for tissue-resident macrophages involved in tissue repair and regeneration, was down-regulated in *Mif-2*$^{-/-}$ mice compared to WT (Fig. 4K, L). To confirm our mRNA expression data, we analyzed the intracellular protein levels of TNFα, MCP1, Arginase1 and TGFβ in ATMs isolated from vWAT by flow cytometry. While we observed *Mif*$^{-/-}$ mice to exhibit a lower presence of TNFα-positive and MCP1-positive ATMs confirming the mRNA expression data, TNFα-positive and MCP1-positive ATMs were neither increased nor decreased in *Mif-2*$^{-/-}$ mice when compared to WT mice. However, *Mif-2*$^{-/-}$ ATMs express elevated levels cytokines TNFα and MCP1 when compared to *Mif-1*$^{-/-}$ ATMs, confirming an important role for MIF in driving a pro-inflammatory phenotype in ATMs (Supplemental Fig. S2A, B). While the FACS data didn't

not show elevated protein levels of anti-inflammatory markers in *Mif*$^{-/-}$ ATMs, we observed a significant decrease of intracellular Arginase1 levels in *Mif-2*$^{-/-}$ ATMs compared to WT ATMs (Supplemental Fig. S2C, D).

Our results indicate that in vWAT MIF and MIF-2 may exert inverse effects on ATM polarization with MIF contributing to an inflammatory phenotype, as characterized by elevated TNFα and MCP1 expression, while MIF-2 may promote a tissue-resident macrophage and anti-inflammatory phenotype involved in tissue regeneration, as characterized by the expression of the signature marker Arginase 1.

## LPS-treated adipocytes of *Mif-2*$^{-/-}$ mice promote BMDM polarization towards an inflammatory phenotype *in vitro*

We hypothesized that the downregulation of MIF-2 in adipocytes during endotoxemia may contribute to the phenotypic switch of adipose macrophages. We therefore collected supernatants from PBS and LPS-stimulated *Mif-2*$^{-/-}$ (n=12) or WT (n=12) adipocytes, incubated them with BMDMs from WT and *Mif-2*$^{-/-}$ mice, and examined macrophage polarization by flow cytometry. We observed that *Mif-2*$^{-/-}$ BMDM treated with the adipocyte-derived supernatants from *Mif-2*$^{-/-}$ adipocytes showed an increased CD11c/CD301-ratio when compared to *Mif-2*$^{-/-}$ BMDM treated by WT adipocytes (Fig. 5A). A similar result was observed when treating WT BMDM with supernatants from LPS-treated *Mif-2*$^{-/-}$ adipocytes (Supplemental Fig. S3B), while PBS-treated *Mif-2*$^{-/-}$ or WT adipocytes did not affect the macrophage phenotype polarization of *Mif-2*$^{-/-}$ or WT BMDM (Supplemental Fig. S3A, C).

## Down-regulation of adipocyte-derived MIF-2 enhances pro-inflammatory macrophage phenotype

LPS administration *i.p.* results in a down-regulation of MIF-2 in adipocytes (Fig. 2C), and genetic deletion of MIF-2 resulted in an increase of pro-inflammatory phenotype polarization of ATMs when treated with LPS (Fig. 4C, D). In the peritoneum, by contrast, MIF-2 levels are elevated after *i.p.* LPS injection. Given that macrophages are a critical cell population with profound effects on the outcome of sepsis, we examined the effect of MIF-2 on the polarization of PMs by flow cytometry. We treated WT, *Mif*$^{-/-}$, and *Mif-2*$^{-/-}$ mice intraperitoneally with 10 mg/kg LPS or PBS as sham control conditions and analyzed the macrophage phenotype polarization after 24h in PMs as well as ATMs. Under sham conditions, the macrophage phenotype does not differ between WT, *Mif*$^{-/-}$, and *Mif-2*$^{-/-}$ mice when examining PMs or ATMs under sham conditions (Supplemental Fig. S4A), but we observed an increase in pro-inflammatory macrophage phenotypes and increase in CD11c/CD301-ratios under endotoxic conditions for both ATMs and PMs in all genotypes (Supplemental Fig. S4B, C) compared to PBS control conditions. The CD11c/CD301-ratio for PMs and ATMs was significantly reduced in *Mif*$^{-/-}$ mice (n=10) and increased in *Mif-2*$^{-/-}$ mice (n=10) when compared to WT (n=10) mice (Fig. 5B). Moreover, CD11c/CD301-ratios of ATMs were significantly higher when compared to PMs in WT and *Mif*$^{-/-}$ mice. In *Mif-2*$^{-/-}$ mice by contrast, no statistical difference between ATMs and PMs upon LPS administration was observed (Fig. 5B). Together, these results indicate that down-

regulation of MIF-2 in adipocytes upon LPS stimulation may contribute to a promotion of pro-inflammatory macrophage phenotype in ATMs.

To gain further insight into the effects on PMs during endotoxemia, we analyzed the presence of two distinct macrophage subsets within the peritoneal cavity. Macrophages were characterized according to their F4/80 expression, with F4/80$^{high}$ and F4/80$^{low}$ subsets according to the published work by Ghosn et al (28). Previous literature has characterized these two co-existing macrophage subsets according to their functions and origin, with F4/80$^{high}$, CD11b$^{+}$ macrophage subset to be of embryonic precursor origin and to exert tissue-resident macrophage functions, while the F4/80$^{low}$, CD11b$^{+}$ macrophage subset seems to be myeloid-cells derived and to be the major source of pro-inflammatory mediators during inflammation (29). The prevalence of the tissue-resident F4/80$^{high}$, CD11b$^{+}$ macrophage subset decreases in response to inflammation, while the levels of the pro-inflammatory F4/80$^{low}$ macrophage subset increases (28). A gating strategy is shown in (Supplemental Fig. S5A-C). After LPS treatment, *Mif*$^{-/-}$ mice exhibit a significantly lower number of F4/80$^{low}$ macrophage subsets compared to WT and *Mif-2*$^{-/-}$ mice, while the levels of F4/80$^{high}$ macrophage population are higher in *Mif*$^{-/-}$ mice compared to WT and *Mif-2*$^{-/-}$ (Supplemental Fig. S5D). Our results suggest that the high levels of pro-inflammatory F4/80$^{low}$ PMs within the peritoneal cavity in WT and *Mif-2*$^{-/-}$ mice after LPS-treatment may explain the increase of a pro-inflammatory macrophage phenotype in PMs, while the higher levels of F4/80$^{high}$ macrophages in *Mif*$^{-/-}$ mice may support an anti-inflammatory phenotype and lower CD11c/CD301 ratio in *Mif*$^{-/-}$ PMs.

## Supernatants of *Mif*$^{-/-}$ vWAT increase 3T3 viability

Adipose tissue inflammation has been shown to impair wound healing and fibroblasts represent a crucial cell type mediating wound repair (30, 31). Hence, we also examined the impact of adipose tissue-derived MIF and MIF-2 in endotoxemia on fibroblast viability in a co-culture assay. Visceral WAT samples after LPS treatment from WT, *Mif*$^{-/-}$, and *Mif-2*$^{-/-}$ mice (in 0.5% FCS medium) were co-cultured with 3T3 fibroblasts, and fibroblast viability was measured by the alamarBlue® assay (n=8). 0.5% FCS medium served as negative control, 10% FCS medium as positive control. Fibroblasts incubated with vWAT of *Mif*$^{-/-}$ mice showed a significantly higher viability when compared to vWAT of WT mice. There was no difference seen between fibroblasts co-cultured with vWAT from *Mif-2*$^{-/-}$ or WT mice (Fig. 5C).

## MIF and MIF-2 are reciprocally regulated in adipose tissue of septic patients

To investigate the potential translation of our mouse model findings to human sepsis, we measured the MIF and MIF-2 protein content of sWAT samples from ten patients suffering from Gram-negative sepsis (6 female, 4 male; mean age: 57.3 ± 4.02 years; mean BMI: 29.96 ± 1.91) and non-septic patients (3 female, 7 male; mean age: 42.5 ± 5.44; mean BMI: 28.56 ± 1.79). Importantly, like the observation in the murine endotoxemia model, MIF was significantly up-regulated in adipose tissue from septic patients (Fig. 6A) whereas MIF-2 was significantly down-regulated (Fig. 6B).

## Discussion

LPS is the main inflammatory component of the external membrane of Gram-negative bacteria, and is responsible for many of the toxic features of the host response to bacteria (32). LPS-induced endotoxemia is commonly used to mimic sepsis as it leads to fulminant systemic inflammation in mice with activation of the innate immune response (33). The role of MIF in LPS induced endotoxemia has been well studied early on and contributes to disease severity (17, 34). Expressed by both pituitary gland cells as well as immune cells throughout the progression of endotoxemia, MIF is vital for the development of an ensuing inflammatory immune response (17, 35). It's contribution to disease severity involves overriding the anti-inflammatory and protective effects of glucocorticoids, recruitment of leukocytes to the site of infection through its chemokine-like functions, and activation of immune cells to produce large amounts of inflammatory cytokines driving inflammation (36, 37). Genetic deletion as well as immunoneutralization through antibodies or small molecule inhibitors against MIF have been shown to protect mice from lethal consequences of sepsis, even when treated several hours after microbial invasion (15). In contrast to MIF, knowledge about the function of MIF-2 in sepsis and endotoxemia is sparse. The action of MIF-2 in LPS shock was investigated by Merk *et al.* earlier who showed that *i.p.* injection of LPS led to elevation of both plasma MIF and MIF-2 levels in mice. MIF-2 secretion also was up-regulated in cultured macrophages with similar kinetics as MIF upon LPS stimulation (16). MIF-2 serum levels also have been reported to be increased in burn patients with sepsis (38).

Obesity is accompanied by a low-grade chronic inflammatory state of adipose tissue, and with an increased content of activated macrophages (39). In contrast to the up-regulation of MIF-2 during sepsis and burn injury (40), MIF-2 was shown to be down-regulated in adipose tissue during obesity and appears to exert an inverse role to MIF with respect to insulin resistance and glucose metabolism. Iwata *et al.* found that contrary to MIF (41), *Mif-2* expression in adipocytes negatively correlates with the patients' BMI and improves obesity induced glucose intolerance. The same group further showed an inhibitory effect of MIF-2 on adipogenesis by interleukin 6 (IL6) (42). We recently reported an inverse regulation of MIF and MIF-2 in human adipose tissue collected from non-healing inflammatory wounds (21, 43), although a limitation of this prior study was that protein and mRNA levels of whole adipose tissue were measured.

In the present work, we digested adipose tissue and identified adipocytes as the main cell type that is responsible for the observed MIF-2 down-regulation upon LPS-induced endotoxemia. This observation is supported by Iwata *et al.* who noted MIF-2 expression only in mature adipocytes but not in adipogenic precursor cells and saw a negative association between adipocytes and the donor's BMI (19). While no increase of MIF-2 in the stromal vascular fraction of WT mice after *in vivo* LPS injection was seen, a significant increase of MIF-2 was observed in SVF cells when treated with LPS *in vitro*. A reason for the increase, which was not observed in SVF cells *in vivo*, could be the differing concentration of LPS used during *in vitro* culture or unknown systemic counter-regulatory mechanisms. We observed that the downregulation of MIF-2 in adipose tissue is linked to adipocytes, while MIF-2 as well as MIF are both up-regulated in the intraperitoneal fluid after LPS injection. While the up-regulation of peritoneal MIF may be linked to elevated infiltration of pro-

inflammatory PMs to the site of inflammation, *Mif-2* expression was not upregulated in PMs, suggesting other cellular sources for peritoneal MIF-2.

Adipose tissue macrophages may contribute to systemic inflammation (44). Macrophages are a dynamic cell type that are often exposed to a large variety of microenvironmental signals such as cytokines, which influence macrophage polarization and activation (45, 46). Some macrophages exhibit a pro-inflammatory phenotype, which are crucial in host-defense against pathogens and promote inflammation by secretion of pro-inflammatory cytokines (47). Other subtypes can be classified as tissue-resident macrophages, which have been described to have immunosuppressive and reparative functions (47). Many studies have also shown that upon changes in the environmental conditions, macrophages can switch from one phenotype to the other (47, 48). The classically defined M1 and M2 macrophage subtypes are now rather considered to represent the extreme phenotypic ends of a continuous and reversible spectrum of macrophage phenotypic identities that are governed by numerous microenvironmental determinants (47). It has been shown that Gram-negative and positive bacteria provoke a pro-inflammatory activation shift of macrophages and thereby aggravate inflammatory processes (49). Studies by Lumeng and colleagues showed an obesity-related shift towards the pro-inflammatory phenotype in WAT (50). Other studies demonstrated the dominance of inflammatory peritoneal macrophages upon *i.p.* LPS administration (51). Throughout this study, we have categorized our macrophages either as pro-inflammatory phenotype with high CD11c expression or as anti-inflammatory phenotype with high CD301 expression. In our study, LPS endotoxemia resulted in a significant increase in pro-inflammatory macrophages in vWAT and in the peritoneum when compared to the respective PBS-treated control groups in WT, *Mif*$^{-/-}$ and *Mif-2*$^{-/-}$ mice. The predominance of pro-inflammatory activated ATMs may fuel systemic inflammation by promoting the release of soluble factors such as TNFα or MCP1 and contribute to a disrupted glucose metabolism, which occurs commonly during septic illness (52). As an up-stream regulator of pro-inflammatory cascades, MIF has been shown in prior studies to promote an inflammatory-polarizing effect on macrophages. During obesity and chronic adipose tissue inflammation, MIF was also reported to polarize ATMs towards a pro-inflammatory phenotype (53–55). These preceding publications are in line with our findings that reveal a shift of ATMs and PMs towards an anti-inflammatory phenotype in *Mif*-deficient mice.

Strikingly, we observed an opposite action of MIF-2, as ATMs and PMs of *Mif-2*$^{-/-}$ mice showed increased CD11c/CD301-ratios when compared to WT mice. Interestingly, the PMs of *Mif*$^{-/-}$ and WT mice showed a consistently lower CD11c/CD301-ratio when compared to ATMs. This difference in the polarization of ATMs and PMs, however, was not seen in *Mif-2*$^{-/-}$ mice which may indicate that the downregulation of MIF-2 specifically in adipocytes contributes to the pro-inflammatory phenotype polarization of ATMs. A more detailed analysis into the PM subset showed lower levels of the myeloid-derived, pro-inflammatory macrophage subset F4/80$^{low}$, CD11b$^{+}$ in the peritoneal cavity of *Mif*$^{-/-}$ mice after LPS-treatment, but an increase in the tissue-resident macrophage subset F4/80$^{high}$, CD11b$^{+}$ compared to WT and *Mif-2*$^{-/-}$ mice. These different macrophage subset distributions may contribute to the anti-inflammatory phenotype and lower CD11c/CD301 ratio we observe in *Mif*$^{-/-}$ PMs.

In line with prior reports, we observed MIF to elevate the mRNA expression as well as the protein levels of TNFα and MCP1 in ATMs (53–55), while we observed MIF-2 to regulate the mRNA expression and intracellular protein levels of Arginase 1. This enzyme has been described as an anti-inflammatory signature marker for macrophages with an involvement in tissue repair and regeneration (56), which may suggest a tissue-protective role for MIF-2.

Wound infections contribute to sepsis, and sepsis itself may impair wound repair (57). The surgeon faces the dilemma of surgically treating septic foci and thereby causing another defect that requires treatment and potentially aggravates the critical status of the patient. Based on studies with severely septic patients, Koskela *et al.* concluded that sepsis delays epidermal restoration (58) and other studies have reported a detrimental effect of systemic inflammation on wound healing (57, 59). In line with our previous study, where we demonstrated an enhancement of fibroblast proliferation in an *in vitro* scratch assay by use of MIF neutralizing antibodies (21), our viability assay results indicate a harmful effect of MIF on fibroblast viability. The viability of cultured 3T3-L1 fibroblasts was significantly increased when co-cultured with vWAT of LPS-injected $Mif^{-/-}$ mice. MIF-2, on the other hand, appeared to have negligible effect on fibroblast viability.

There are some limitations to our mouse and *in vitro* studies. We only discerned between adipocytes and SVF cells. The SVF, however, is a heterogeneous mix of cells so that a more precise characterization of cell types may reveal a more complex regulation of MIF and MIF-2. Furthermore, the *in vitro* wound healing experiments should be supported by additional *in vivo* investigations in the future. While we selected *β-actin* as a housekeeping gene for our gene expression experiments due to its stable expression profile, other reference genes would be suitable as well. We also used BMDMs instead of ATMs for the *in vitro* polarization experiments as the isolation and cultivation of BMDMs was easier and more consistent when compared to ATMs.

Finally, the analysis of WAT samples from patients suffering from Gram-negative sepsis suggests that the results of these murine studies are applicable to human physiology. The results also confirmed that not only local adipose tissue inflammation (21, 43) but also systemic inflammatory conditions lead to a reciprocal regulation of MIF and MIF-2 in humans.

Our primary goal of the present study was to understand MIF and MIF-2 function in sepsis in lean mice. In the next step, their respective roles in sepsis under obese conditions will be investigated.

## Conclusion

MIF and MIF-2 are differentially regulated in vWAT during LPS endotoxemia and Gram-negative sepsis. Simultaneously elevated levels of MIF as well as a decreased production of MIF-2 lead to an increased polarization of ATMs towards a pro-inflammatory phenotype in adipose tissue. Increased numbers of pro-inflammatory macrophages in the adipose tissue may further drive the septic-dysregulated immune response by excessive inflammatory cytokine production.

## Supplementary Material

Refer to Web version on PubMed Central for supplementary material.

## Acknowledgments

We thank Dr. Omar El Bounkari from the Department of Vascular Biology, Institute for Stroke and Dementia Research, Ludwig-Maximilians-University Munich and Dr. Epameinondas Gousopoulos from the Department of Plastic Surgery and Hand Surgery, University Hospital Zurich, Switzerland for their assistance in the revision of the manuscript.

The authors were supported by funding from the Deutsche Forschungsgemeinschaft (DFG): SCHU2851/1-1 (W.S.), KI1973/1-1 and KI1973/2-1 (B.S.K.), SFB 1123/A03, BE1977/7-1, and BE1977/11-1 (J.B.); by the START program of RWTH Aachen University 691346, START 2013-2 (B.S.K.), by NIH grants AR049610, HL130669 (R.B.) and by an Arthritis Foundation Award 548970 (P.V.T.). W.S. is participant in the BIH Charité Clinician Scientist Program funded by the Charité - Universitätsmedizin Berlin and the Berlin Institute of Health.

## Abbreviation:

| | |
|---|---|
| **MIF** | Macrophage Migration Inhibitory Factor |
| **MIF-2** | Macrophage Migration Inhibitory Factor 2 |
| **D-DT** | D-Dopachrome Tautomerase |
| **LPS** | Lipopolysaccharide |
| **vWAT** | visceral White Adipose Tissue |
| **ATM** | Adipose Tissue Macrophages |
| **BMDM** | Bone Marrow-Derived Macrophages |
| **PM** | Peritoneal Macrophages |

## References:

1. Martin GS (2012) Sepsis, severe sepsis and septic shock: changes in incidence, pathogens and outcomes. Expert Rev Anti Infect Ther 10, 701–706 [PubMed: 22734959]
2. Vincent JL, Marshall JC, Namendys-Silva SA, Francois B, Martin-Loeches I, Lipman J, Reinhart K, Antonelli M, Pickkers P, Njimi H, Jimenez E, Sakr Y, and investigators I (2014) Assessment of the worldwide burden of critical illness: the intensive care over nations (ICON) audit. Lancet Respir Med 2, 380–386 [PubMed: 24740011]
3. (1992) American College of Chest Physicians/Society of Critical Care Medicine Consensus Conference: definitions for sepsis and organ failure and guidelines for the use of innovative therapies in sepsis. Crit Care Med 20, 864–874 [PubMed: 1597042]
4. (2016) Sepsis and septic shock. Nat Rev Dis Primers 2, 16046 [PubMed: 27357137]
5. Iwashyna TJ, Ely EW, Smith DM, and Langa KM (2010) Long-term cognitive impairment and functional disability among survivors of severe sepsis. JAMA 304, 1787–1794 [PubMed: 20978258]
6. Hecker A, Reichert M, Reuss CJ, Schmoch T, Riedel JG, Schneck E, Padberg W, Weigand MA, and Hecker M (2019) Intra-abdominal sepsis: new definitions and current clinical standards. Langenbecks Arch Surg
7. Hillenbrand A, Knippschild U, Weiss M, Schrezenmeier H, Henne-Bruns D, Huber-Lang M, and Wolf AM (2010) Sepsis induced changes of adipokines and cytokines - septic patients compared to morbidly obese patients. BMC surgery 10, 26 [PubMed: 20825686]

8. Kolyva AS, Zolota V, Mpatsoulis D, Skroubis G, Solomou EE, Habeos IG, Assimakopoulos SF, Goutzourelas N, Kouretas D, and Gogos CA (2014) The role of obesity in the immune response during sepsis. Nutr Diabetes 4, e137 [PubMed: 25244356]
9. Pepper DJ, Sun J, Welsh J, Cui X, Suffredini AF, and Eichacker PQ (2016) Increased body mass index and adjusted mortality in ICU patients with sepsis or septic shock: a systematic review and meta-analysis. Crit Care 20, 181 [PubMed: 27306751]
10. Wang S, Liu X, Chen Q, Liu C, Huang C, and Fang X (2017) The role of increased body mass index in outcomes of sepsis: a systematic review and meta-analysis. BMC anesthesiology 17, 118 [PubMed: 28859605]
11. Dickerson RN (2013) The obesity paradox in the ICU: real or not? Crit Care 17, 154 [PubMed: 23758984]
12. Nishimura S, Manabe I, Nagasaki M, Eto K, Yamashita H, Ohsugi M, Otsu M, Hara K, Ueki K, Sugiura S, Yoshimura K, Kadowaki T, and Nagai R (2009) CD8+ effector T cells contribute to macrophage recruitment and adipose tissue inflammation in obesity. Nature medicine 15, 914–920
13. Merk M, Mitchell RA, Endres S, and Bucala R (2012) D-dopachrome tautomerase (D-DT or MIF-2): doubling the MIF cytokine family. Cytokine 59, 10–17 [PubMed: 22507380]
14. Bloom BR, and Bennett B (1966) Mechanism of a reaction in vitro associated with delayed-type hypersensitivity. Science 153, 80–82 [PubMed: 5938421]
15. Calandra T, Echtenacher B, Roy DL, Pugin J, Metz CN, Hultner L, Heumann D, Mannel D, Bucala R, and Glauser MP (2000) Protection from septic shock by neutralization of macrophage migration inhibitory factor. Nat Med 6, 164–170 [PubMed: 10655104]
16. Merk M, Zierow S, Leng L, Das R, Du X, Schulte W, Fan J, Lue H, Chen Y, Xiong H, Chagnon F, Bernhagen J, Lolis E, Mor G, Lesur O, and Bucala R (2011) The D-dopachrome tautomerase (DDT) gene product is a cytokine and functional homolog of macrophage migration inhibitory factor (MIF). Proc Natl Acad Sci U S A 108, E577–585 [PubMed: 21817065]
17. Bernhagen J, Calandra T, Mitchell RA, Martin SB, Tracey KJ, Voelter W, Manogue KR, Cerami A, and Bucala R (1993) MIF is a pituitary-derived cytokine that potentiates lethal endotoxaemia. Nature 365, 756–759 [PubMed: 8413654]
18. Kim BS, Pallua N, Bernhagen J, and Bucala R (2015) The macrophage migration inhibitory factor protein superfamily in obesity and wound repair. Experimental & molecular medicine 47, e161 [PubMed: 25930990]
19. Iwata T, Taniguchi H, Kuwajima M, Taniguchi T, Okuda Y, Sukeno A, Ishimoto K, Mizusawa N, and Yoshimoto K (2012) The action of D-dopachrome tautomerase as an adipokine in adipocyte lipid metabolism. PloS one 7, e33402
20. Kim BS, Tilstam PV, Hwang SS, Simons D, Schulte W, Leng L, Sauler M, Ganse B, Averdunk L, Kopp R, Stoppe C, Bernhagen J, Pallua N, and Bucala R (2017) D-dopachrome tautomerase in adipose tissue inflammation and wound repair. Journal of cellular and molecular medicine 21, 35–45 [PubMed: 27605340]
21. Kim BS, Rongisch R, Hager S, Grieb G, Nourbakhsh M, Rennekampff HO, Bucala R, Bernhagen J, and Pallua N (2015) Macrophage Migration Inhibitory Factor in Acute Adipose Tissue Inflammation. PLoS One 10, e0137366
22. Fingerle-Rowson G, Petrenko O, Metz CN, Forsthuber TG, Mitchell R, Huss R, Moll U, Muller W, and Bucala R (2003) The p53-dependent effects of macrophage migration inhibitory factor revealed by gene targeting. Proc Natl Acad Sci U S A 100, 9354–9359 [PubMed: 12878730]
23. Qi D, Atsina K, Qu L, Hu X, Wu X, Xu B, Piecychna M, Leng L, Fingerle-Rowson G, Zhang J, Bucala R, and Young LH (2014) The vestigial enzyme D-dopachrome tautomerase protects the heart against ischemic injury. J Clin Invest 124, 3540–3550 [PubMed: 24983315]
24. Cho KW, Morris DL, and Lumeng CN (2014) Flow cytometry analyses of adipose tissue macrophages. Methods in enzymology 537, 297–314 [PubMed: 24480353]
25. Moustaid N, Jones BH, and Taylor JW (1996) Insulin increases lipogenic enzyme activity in human adipocytes in primary culture. J Nutr 126, 865–870 [PubMed: 8613889]
26. Weischenfeldt J, and Porse B (2008) Bone Marrow-Derived Macrophages (BMM): Isolation and Applications. CSH Protoc 2008, pdb prot5080

27. Bone RC, Sibbald WJ, and Sprung CL (1992) The ACCP-SCCM consensus conference on sepsis and organ failure. Chest 101, 1481–1483 [PubMed: 1600757]
28. Ghosn EE, Cassado AA, Govoni GR, Fukuhara T, Yang Y, Monack DM, Bortoluci KR, Almeida SR, Herzenberg LA, and Herzenberg LA (2010) Two physically, functionally, and developmentally distinct peritoneal macrophage subsets. Proc Natl Acad Sci U S A 107, 2568–2573 [PubMed: 20133793]
29. Cassado Ados A, D'Imperio Lima MR, and Bortoluci KR (2015) Revisiting mouse peritoneal macrophages: heterogeneity, development, and function. Front Immunol 6, 225 [PubMed: 26042120]
30. Pierpont YN, Dinh TP, Salas RE, Johnson EL, Wright TG, Robson MC, and Payne WG (2014) Obesity and surgical wound healing: a current review. ISRN Obes 2014, 638936
31. Bainbridge P (2013) Wound healing and the role of fibroblasts. J Wound Care 22, 407–408, 410–412 [PubMed: 23924840]
32. Ayala A, and Chaudry IH (1996) Immune dysfunction in murine polymicrobial sepsis: mediators, macrophages, lymphocytes and apoptosis. Shock 6 Suppl 1, S27–38 [PubMed: 8828095]
33. Fink MP Animal models of sepsis. Virulence 5, 143–153 [PubMed: 24022070]
34. Roger T, Glauser MP, and Calandra T (2001) Macrophage migration inhibitory factor (MIF) modulates innate immune responses induced by endotoxin and Gram-negative bacteria. J Endotoxin Res 7, 456–460 [PubMed: 11753217]
35. Calandra T, Spiegel LA, Metz CN, and Bucala R (1998) Macrophage migration inhibitory factor is a critical mediator of the activation of immune cells by exotoxins of Gram-positive bacteria. Proc Natl Acad Sci U S A 95, 11383–11388 [PubMed: 9736745]
36. Flaster H, Bernhagen J, Calandra T, and Bucala R (2007) The macrophage migration inhibitory factor-glucocorticoid dyad: regulation of inflammation and immunity. Mol Endocrinol 21, 1267–1280 [PubMed: 17389748]
37. Grieb G, Merk M, Bernhagen J, and Bucala R (2010) Macrophage migration inhibitory factor (MIF): a promising biomarker. Drug News Perspect 23, 257–264 [PubMed: 20520854]
38. Kim BS, Stoppe C, Grieb G, Leng L, Sauler M, Assis D, Simons D, Boecker AH, Schulte W, Piecychna M, Hager S, Bernhagen J, Pallua N, and Bucala R The clinical significance of the MIF homolog d-dopachrome tautomerase (MIF-2) and its circulating receptor (sCD74) in burn. Burns
39. Hotamisligil GS, Shargill NS, and Spiegelman BM (1993) Adipose expression of tumor necrosis factor-alpha: direct role in obesity-linked insulin resistance. Science 259, 87–91 [PubMed: 7678183]
40. Kim BS, Stoppe C, Grieb G, Leng L, Sauler M, Assis D, Simons D, Boecker AH, Schulte W, Piecychna M, Hager S, Bernhagen J, Pallua N, and Bucala R (2016) The clinical significance of the MIF homolog d-dopachrome tautomerase (MIF-2) and its circulating receptor (sCD74) in burn. Burns 42, 1265–1276 [PubMed: 27209369]
41. Skurk T, Herder C, Kraft I, Muller-Scholze S, Hauner H, and Kolb H (2005) Production and release of macrophage migration inhibitory factor from human adipocytes. Endocrinology 146, 1006–1011 [PubMed: 15576462]
42. Ishimoto K, Iwata T, Taniguchi H, Mizusawa N, Tanaka E, and Yoshimoto K D-dopachrome tautomerase promotes IL-6 expression and inhibits adipogenesis in preadipocytes. Cytokine 60, 772–777 [PubMed: 22951300]
43. Kim BS, Tilstam PV, Hwang SS, Simons D, Schulte W, Leng L, Sauler M, Ganse B, Averdunk L, Kopp R, Stoppe C, Bernhagen J, Pallua N, and Bucala R (2016) D-dopachrome tautomerase in adipose tissue inflammation and wound repair. J Cell Mol Med
44. Morris DL, Cho KW, Delproposto JL, Oatmen KE, Geletka LM, Martinez-Santibanez G, Singer K, and Lumeng CN Adipose tissue macrophages function as antigen-presenting cells and regulate adipose tissue CD4+ T cells in mice. Diabetes 62, 2762–2772
45. Gordon S (2003) Alternative activation of macrophages. Nat Rev Immunol 3, 23–35 [PubMed: 12511873]
46. Gordon S, and Taylor PR (2005) Monocyte and macrophage heterogeneity. Nat Rev Immunol 5, 953–964 [PubMed: 16322748]

47. Atri C, Guerfali FZ, and Laouini D (2018) Role of Human Macrophage Polarization in Inflammation during Infectious Diseases. Int J Mol Sci 19

48. Italiani P, Mazza EM, Lucchesi D, Cifola I, Gemelli C, Grande A, Battaglia C, Bicciato S, and Boraschi D (2014) Transcriptomic profiling of the development of the inflammatory response in human monocytes in vitro. PLoS One 9, e87680

49. Benoit M, Desnues B, and Mege JL (2008) Macrophage polarization in bacterial infections. J Immunol 181, 3733–3739 [PubMed: 18768823]

50. Lumeng CN, Bodzin JL, and Saltiel AR (2007) Obesity induces a phenotypic switch in adipose tissue macrophage polarization. J Clin Invest 117, 175–184 [PubMed: 17200717]

51. Ni Gabhann J, Hams E, Smith S, Wynne C, Byrne JC, Brennan K, Spence S, Kissenpfennig A, Johnston JA, Fallon PG, and Jefferies CA Btk regulates macrophage polarization in response to lipopolysaccharide. PLoS One 9, e85834

52. Van Cromphaut SJ, Vanhorebeek I, and Van den Berghe G (2008) Glucose metabolism and insulin resistance in sepsis. Curr Pharm Des 14, 1887–1899 [PubMed: 18691100]

53. Heinrichs D, Berres ML, Coeuru M, Knauel M, Nellen A, Fischer P, Philippeit C, Bucala R, Trautwein C, Wasmuth HE, and Bernhagen J (2014) Protective role of macrophage migration inhibitory factor in nonalcoholic steatohepatitis. FASEB journal : official publication of the Federation of American Societies for Experimental Biology 28, 5136–5147 [PubMed: 25122558]

54. Finucane OM, Reynolds CM, McGillicuddy FC, Harford KA, Morrison M, Baugh J, and Roche HM Macrophage migration inhibitory factor deficiency ameliorates high-fat diet induced insulin resistance in mice with reduced adipose inflammation and hepatic steatosis. PLoS One 9, e113369

55. Verschuren L, Kooistra T, Bernhagen J, Voshol PJ, Ouwens DM, van Erk M, de Vries-van der Weij J, Leng L, van Bockel JH, van Dijk KW, Fingerle-Rowson G, Bucala R, and Kleemann R (2009) MIF deficiency reduces chronic inflammation in white adipose tissue and impairs the development of insulin resistance, glucose intolerance, and associated atherosclerotic disease. Circ Res 105, 99–107 [PubMed: 19478200]

56. Campbell L, Saville CR, Murray PJ, Cruickshank SM, and Hardman MJ (2013) Local arginase 1 activity is required for cutaneous wound healing. J Invest Dermatol 133, 2461–2470 [PubMed: 23552798]

57. Rico RM, Ripamonti R, Burns AL, Gamelli RL, and DiPietro LA (2002) The effect of sepsis on wound healing. The Journal of surgical research 102, 193–197 [PubMed: 11796018]

58. Koskela M, Gaddnas F, Ala-Kokko TI, Laurila JJ, Saarnio J, Oikarinen A, and Koivukangas V (2009) Epidermal wound healing in severe sepsis and septic shock in humans. Crit Care 13, R100 [PubMed: 19552820]

59. Sommer K, Sander AL, Albig M, Weber R, Henrich D, Frank J, Marzi I, and Jakob H (2013) Delayed wound repair in sepsis is associated with reduced local pro-inflammatory cytokine expression. PloS one 8, e73992

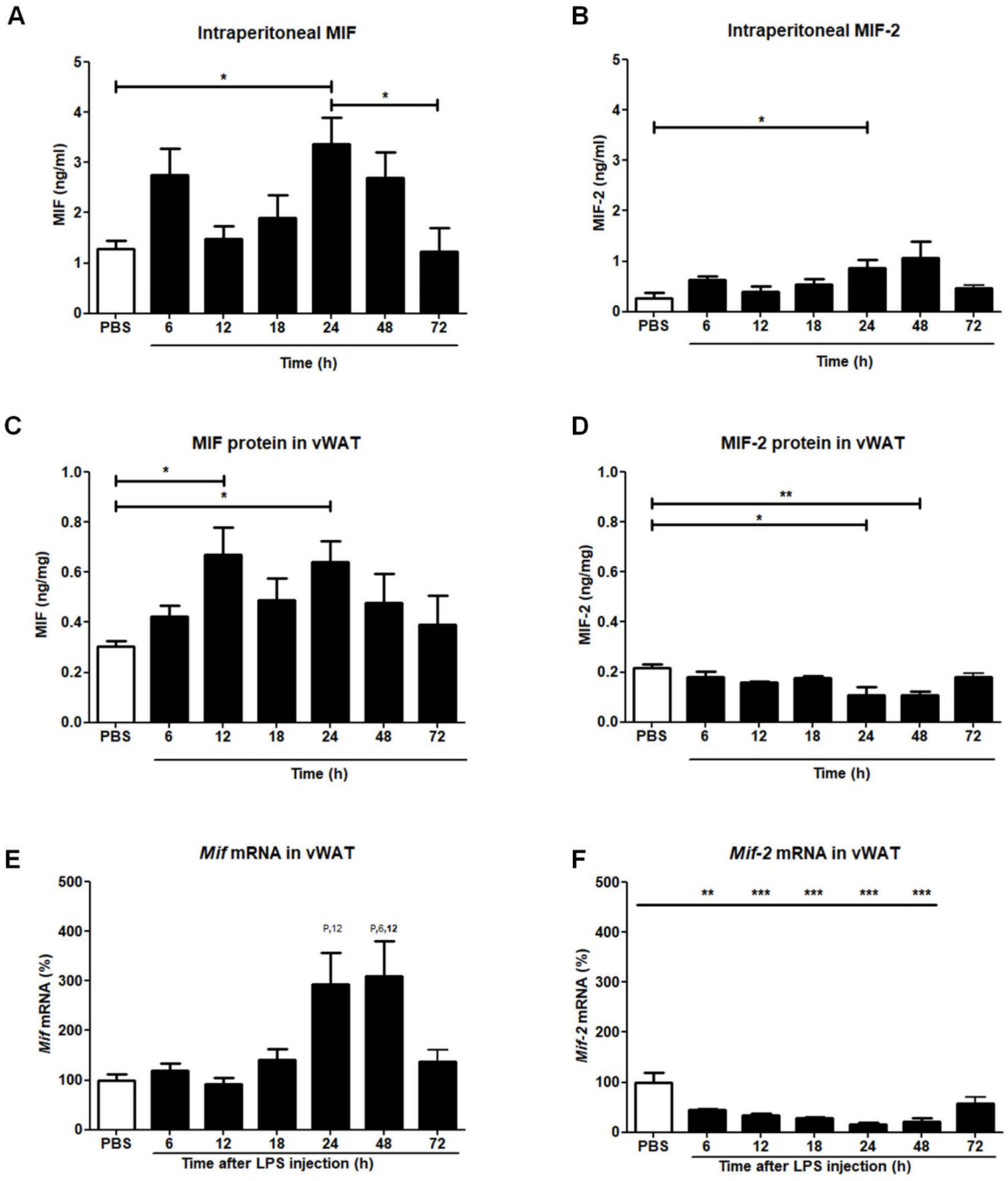


**Figure 1: Peritoneal and adipose MIF and MIF-2 levels in endotoxemia.**

WT mice were injected with 10 mg/kg LPS intraperitoneally. Intraperitoneal fluid or vWAT were harvested 6, 12, 18, 24, 48, and 72 hours (n=8 per group) after LPS injection. MIF or MIF-2 levels were determined by quantitative RT-PCR or ELISA. PBS injected mice served as controls. **(A)** Intraperitoneal MIF protein levels **(B)** Intraperitoneal MIF-2 protein levels **(C)** MIF protein levels in vWAT **(D)** MIF-2 protein levels in vWAT **(E)** *Mif* mRNA expression in vWAT **(F)** *Mif-2* mRNA expression in vWAT. Statistically significant differences are indicated by asterisks (* $p < 0.05$; ** $p < 0.01$; *** $p < 0.001$); in Figure 1E:

not bold/not italicized: $p < 0.05$; bold/not italicized: $p < 0.01$. p: PBS, 6: 6h, 12: 12h, 18: 18h, 72: 72h.

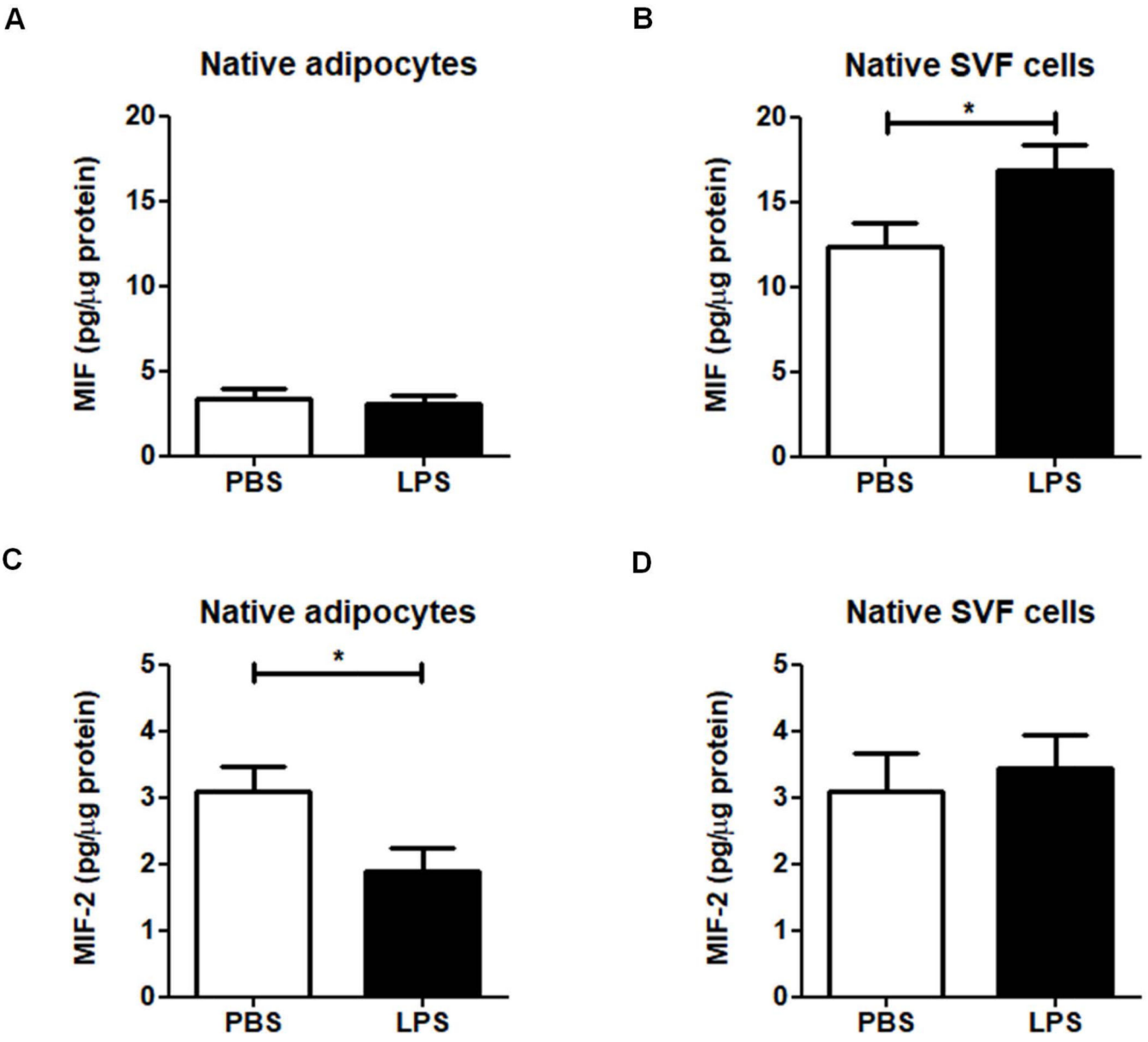


**Figure 2: MIF and MIF-2 protein levels in native adipocytes and SVF cells.**

Visceral WAT was digested by collagenase to separate adipocytes from the SVF (n=8). In **(A)** and **(B)**, MIF protein was measured in adipocytes and SVF cells from WT mice 24h after *i.p.* injection of 10 mg/kg LPS. In **(C)** and **(D)** MIF-2 protein was measured in adipocytes and SVF cells isolated from WT mice 24h after *i.p.* injection of 10 mg/kg LPS. Statistically significant differences are indicated by asterisks (* $p < 0.05$).

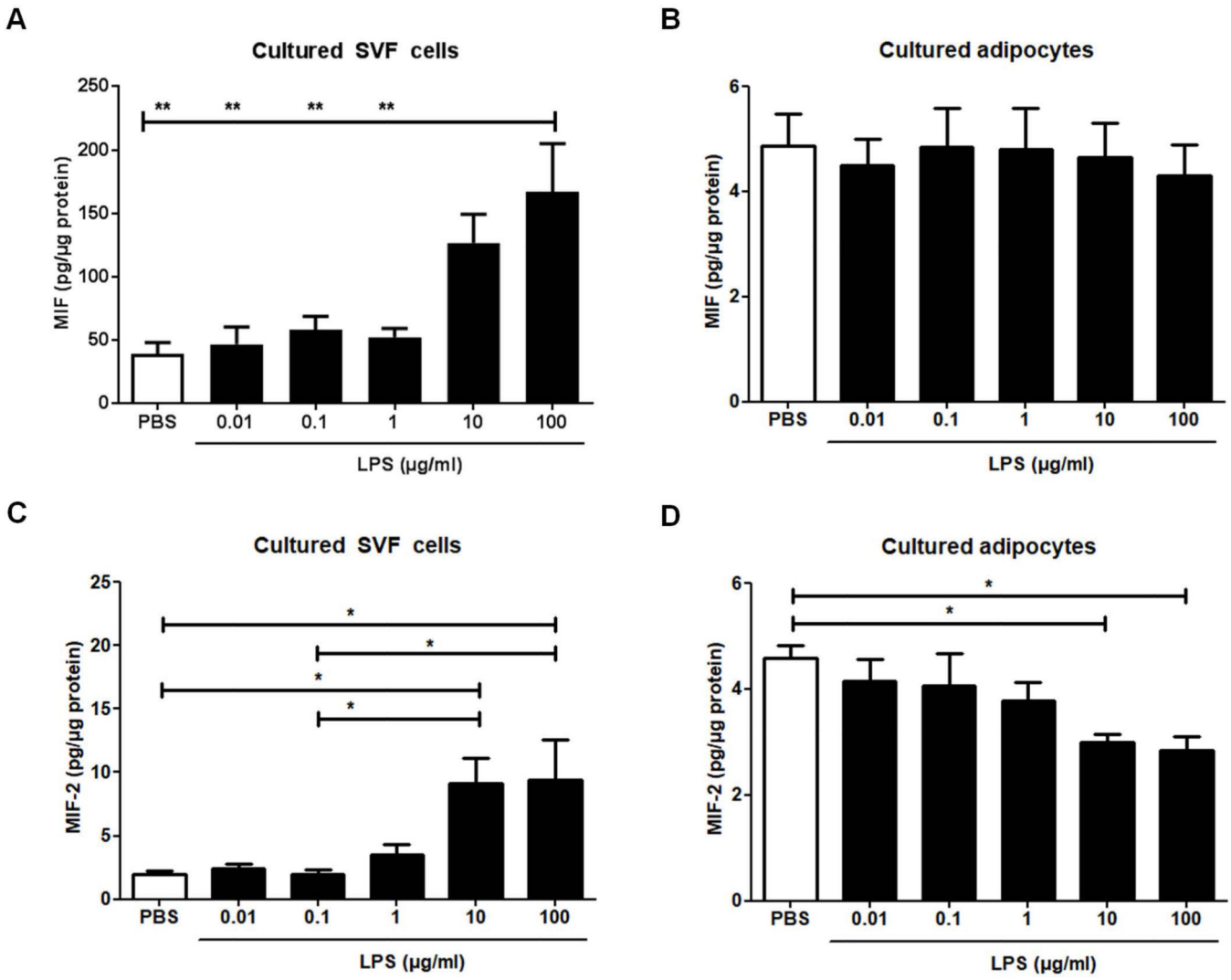


**Figure 3: MIF and MIF-2 protein levels in cultured adipocytes and SVF cells.**

Adipocytes and SVF were isolated from vWAT from WT mice (n=6) and stimulated *in vitro* with different concentrations of LPS. In **(A)** and **(B)** MIF protein levels were measured in the cell supernatant from SVF and adipocytes by ELISA. In **(C)** and **(D)** MIF-2 protein levels were measured in the cell supernatant from SVF and adipocytes by ELISA. Statistically significant differences are indicated by asterisks (* $p < 0.05$; ** $p < 0.01$).

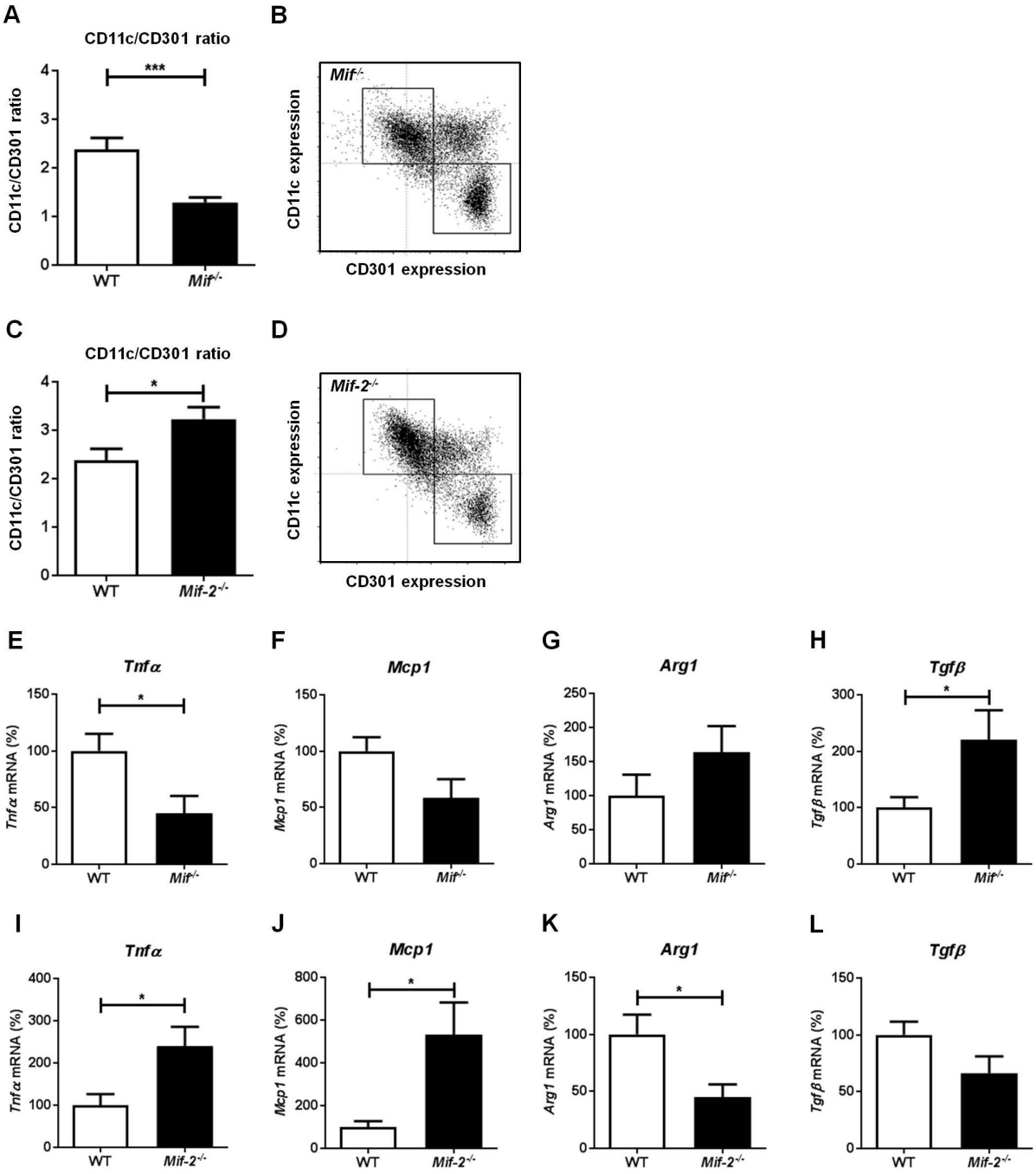


**Figure 4: ATM polarization in *Mif*$^{-/-}$ and *Mif-2*$^{-/-}$ mice in endotoxemia.**

*Mif*$^{-/-}$, *Mif-2*$^{-/-}$ and WT mice were injected with 10 mg/kg LPS intraperitoneally and vWAT was harvested after 24h. Visceral WAT was digested by collagenase and the SVF underwent flow cytometry analysis. Pro-inflammatory ATMs were defined as CD45$^{+}$, CD11b$^{+}$, F4/80$^{+}$, CD11c$^{+}$ cells and anti-inflammatory ATMs were defined as CD45$^{+}$, CD11$^{+}$, F4/80$^{+}$, CD301$^{+}$ cells. The relative CD11c/CD301-ratio was measured by flow cytometry. **(A,B)** Ratios were compared between *Mif*$^{-/-}$ and WT mice (n=10 each group) with representative flow plots shown in **(B)**, and **(C,D)** between WT and *Mif-2*$^{-/-}$ mice

(n=10 each group) with representative flow plots shown in **(D)**. **(E-H)** mRNA expression (n=8 each group) of pro-inflammatory macrophage phenotype typical genes of **(E)** *Tnfa*, **(F)** *Mcp1*, and anti-inflammatory macrophage phenotype related genes **(G)** *Arg1* and **(H)** *Tgfβ* isolated from vWAT were measured by quantitative RT-PCR and compared between *Mif*$^{-/-}$ and WT mice. **(I-L)** mRNA expression of pro-inflammatory macrophage phenotype typical genes of **(I)** *Tnfa*, **(J)** *Mcp1*, and anti-inflammatory macrophage phenotype related genes **(K)** *Arg1* and **(L)** *Tgfβ* isolated from vWAT were measured by quantitative RT-PCR and compared between *Mif-2*$^{-/-}$ and WT mice. Statistically significant differences are indicated by asterisks (* $p < 0.05$, *** $p < 0.001$).

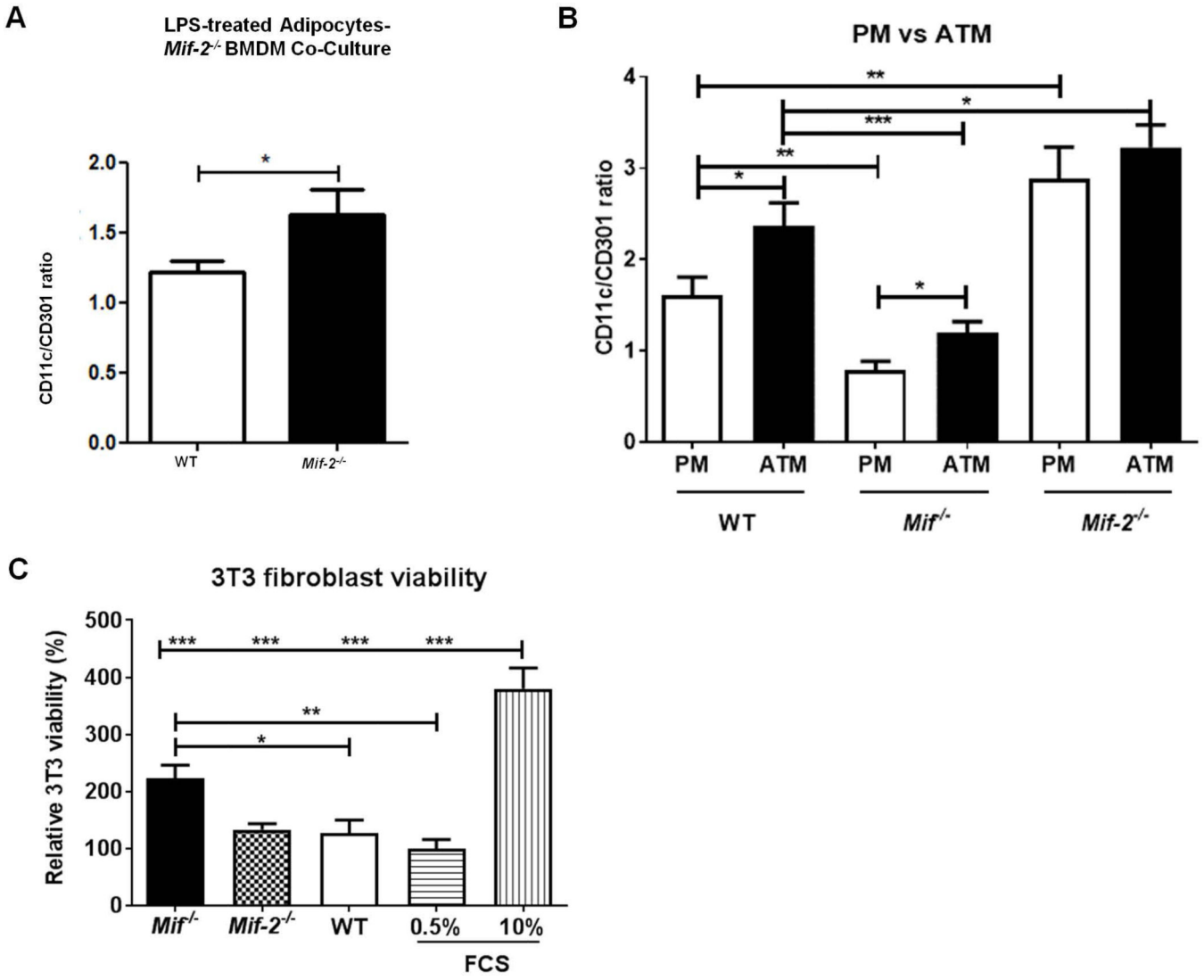


**Figure 5: The effect of adipocyte-derived MIF-2 on macrophage phenotype polarization and the effect of *Mif* and *Mif-2* knockout on fibroblast viability.**

**(A)** *Mif-2*$^{-/-}$ BMDM were treated with supernatants of LPS-stimulated adipocytes of *Mif-2*$^{-/-}$ (n=12) and WT (n=12) mice and *Mif-2*$^{-/-}$ BMDM polarization was assessed by flow cytometry and expressed by the CD11c/CD301-ratio. **(B)** WT, *Mif*$^{-/-}$, and *Mif-2*$^{-/-}$ mice (n=10 each group) were injected intraperitoneally with 10 mg/kg, PMs were isolated by peritoneal lavage and ATMs were collected by collagenase digestion from isolated vWAT. The relative CD11c/CD301-ratio of PMs and ATMs were compared by flow cytometry. Pro-inflammatory macrophages were defined as CD45$^{+}$, CD11b$^{+}$, F4/80$^{+}$, CD11c$^{+}$ cells, while an anti-inflammatory macrophage phenotype was defined as CD45$^{+}$, CD11b$^{+}$, F4/80$^{+}$, CD301$^{+}$ cells. **(C)** Visceral WAT after *i.p.* injection of 10 mg/kg LPS into WT, *Mif*$^{-/-}$, and *Mif-2*$^{-/-}$ mice were explanted after 24h (n=8), co-cultured with 3T3 fibroblasts and fibroblast viability was measured by the alamarBlue® assay. Statistically significant differences are indicated by asterisks (* $p < 0.05$; ** $p < 0.01$; *** $p < 0.001$).

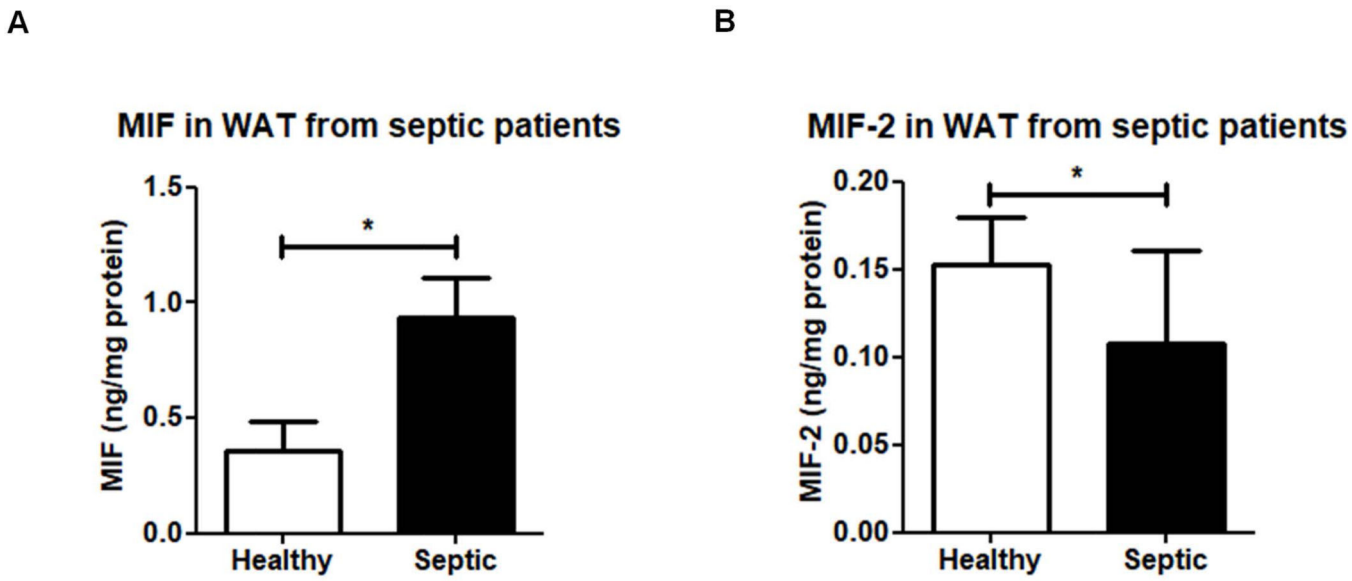


**Figure 6: MIF and MIF-2 protein levels in patients with Gram-negative sepsis.**

Subcutaneous WAT samples were collected from septic patients (n=10) and healthy patients (n=10). Adipose tissue was homogenized, and MIF and MIF-2 protein levels were measured by ELISA. **(A)** MIF protein levels **(B)** MIF-2 protein levels. Statistically significant differences are indicated by asterisks (* $p < 0.05$)

**Table 1**

List of primers used for quantitative real time PCR.

| Gene | *F/R* | Primer Sequence 5' – 3' |
|---|---|---|
| mouse *β-actin* | *F* | GGC-TGT-ATT-CCC-CTC-CAT-CG |
| | *R* | CCA-GTT-GGT-AAC-AAT-GCC-ATG-T |
| mouse *Arg1* | *F* | GGA-ATC-TGC-ATG-GGC-AAC-CTG-TGT |
| | *R* | GGG-TCT-ACG-TCT-CGC-AAG-CCA |
| mouse *Mcp1* | *F* | TGG-AGC-ATC-CAC-GTG-TTG-GC |
| | *R* | ACT-ACA-GCT-TCT-TTG-GGA-CA |
| mouse *Mif* | *F* | CCA-TGC-CTA-TGT-TCA-TCG-TG |
| | *R* | GTG-AAT-GGA-CGT-GGC-GAC-AAG |
| mouse *Mif-2* | *F* | CTC-TTC-TCC-CGC-TAA-CAT-GC |
| | *R* | TCA-TGC-CAG-GTC-GTA-TCG-TA |
| mouse *Tgfβ* | *F* | GGA-GAG-CCC-TGG-ATA-CCA-AC |
| | *R* | CAA-CCC-AGG-TCC-TTC-CTA-AA |
| mouse *Tnfα* | *F* | CCA-GAC-CCT-CAC-ACT-CAG-ATC |